Tropical Rainfall Associated with Convective and Stratiform Clouds: Intercomparison of Disdrometer and Profiler Measurements

ALI TOKAY AND DAVID A. SHORT

Tropical Rainfall Measuring Mission Office, NASA/Goddard Space Flight Center, Greenbelt, Maryland

CHRISTOPHER R. WILLIAMS AND WARNER L. ECKLUND

Cooperative Institute for Research in Environmental Sciences (CIRES), University of Colorado, Boulder, Colorado

KENNETH S. GAGE

NOAA Aeronomy Laboratory, Boulder, Colorado

(Manuscript received 30 December 1996, in final form 20 April 1998)

ABSTRACT

The motivation for this research is to move in the direction of improved algorithms for the remote sensing of rainfall, which are crucial for meso- and large-scale circulation studies and climate applications through better determinations of precipitation type and latent heating profiles. Toward this end a comparison between two independent techniques, designed to classify precipitation type from 1) a disdrometer and 2) a 915-MHz wind profiler, is presented, based on simultaneous measurements collected at the same site during the Intensive Observing Period of the Tropical Ocean Global Atmosphere Coupled Ocean–Atmosphere Response Experiment. Disdrometer-derived quantities such as differences in drop size distribution parameters, particularly the intercept parameter N_0 and rainfall rate, were used to classify rainfall as stratiform or convective. At the same time, profiler-derived quantities, namely, Doppler velocity, equivalent reflectivity, and spectral width, from Doppler spectra were used to classify precipitation type in four categories: shallow convective, deep convective, mixed convective–stratiform, and stratiform.

Overall agreement between the two algorithms is found to be reasonable. Given the disdrometer stratiform classification, the mean profile of reflectivity shows a distinct bright band and associated large vertical gradient in Doppler velocity, both indicators of stratiform rain. For the disdrometer convective classification the mean profile of reflectivity lacks a bright band, while the vertical gradient in Doppler velocity below the melting level is opposite to the stratiform case. Given the profiler classifications, in the order shallow–deep–mixed–stratiform, the composite raindrop spectra for a rainfall rate of 5 mm h^{-1} show an increase in D_0, the median volume diameter, consistent with the dominant microphysical processes responsible for drop formation. Nevertheless, the intercomparison does reveal some limitations in the classification methodology utilizing the disdrometer or profiler algorithms in isolation. In particular, 1) the disdrometer stratiform classification includes individual cases in which the vertical profiles appear convective, but these usually occur at times when the disdrometer classification is highly variable; 2) the profiler classification scheme also appears to classify precipitation too frequently as stratiform by including cases that have small vertical Doppler velocity gradients at the melting level but no bright band; and 3) the profiler classification scheme includes a category of mixed (stratiform–convective) precipitation that has some features in common with deep convection (e.g., enhanced spectral width above the melting level) but other features in common with stratiform precipitation (e.g., well-developed melting layer signature). Comparison of the profiler-derived vertical structure with disdrometer-determined rain rates reveals that almost all cases of rain rates greater than 10 mm h^{-1} are convective. For rain rates less than 5 mm h^{-1} all four profiler-determined precipitation classes are well represented.

1. Introduction

The processes of hydrometeor formation, growth, transformation, and decay occur on a microphysical scale within a larger, cloud-scale environment. The complex chain of processes results in hydrometeor distributions that retain characteristic signatures of the environment in which they have evolved. Radar remote sensing studies have shown that effects of microphysical processes on the hydrometeor size distribution significantly impact the interpretation of remotely sensed data (Waldvogel 1974; Heinrich et al. 1996). While the drop size distribution (DSD) in both heavy and light rain has been given special attention (e.g.,

Corresponding author address: Dr. Ali Tokay, NASA/Goddard Space Flight Center, Code 910.1, Greenbelt, MD 20771.
E-mail: tokay@eas.slu.edu

Willis and Tattleman 1989; Rogers et al. 1991), and numerous studies have been made of DSDs in various climatic regimes (Kodaira and Aoyagi 1990; Battan 1973), more recent studies have strongly suggested the coexistence of distinctly different convective and stratiform DSDs within tropical systems (Tokay and Short 1996, TS hereafter; Marks et al. 1999, manuscript submitted to *J. Appl. Meteor.*). In addition, the recent modeling study of Ferrier et al. (1995) showed that a reparameterization of the DSD into separate convective and stratiform families had a significant impact on model performance. It is evident that the hydrometeor size distribution is central to both remote sensing and modeling studies and that both fields stand to gain from self-consistent, transportable parameterization schemes. It is toward that end that the present study was undertaken.

The convective and stratiform modes of rainfall are especially important in the Tropics, where precipitating clouds often organize into mesoscale systems containing the two distinctive environments (Houze 1989). Within the convective environment, cloud droplets formed in narrow updrafts by the warm-rain processes of nucleation, condensation, and coalescence provide the major source of water for raindrops via continuation of the coalescence process. Microphysical processes such as freezing and riming occur when updrafts carry liquid hydrometeors well above the freezing level, while vapor deposition and aggregation are the dominant ice-phase mechanisms of growth. Those hydrometeors that return to the surface as precipitation are almost always in the liquid phase, especially over the tropical oceans. The resulting convective rainfall is intense, relatively short in duration, and highly fluctuating. Deep convection transports copious amounts of water vapor and cloud particles well above the freezing level where ice nucleation processes, wind shear, detrainment, and gravitational settling create the stratiform environment, as characterized by a large horizontal extent, weak updrafts, ice-crystal growth, and aggregation above the 0°C isotherm and melting and evaporation below. The intensity of stratiform rain is, on average, less than convective rain, but it can persist for hours, resulting in significant rain accumulation. The distinction between convective and stratiform is important dynamically because the differing vertical profiles of latent heating and associated divergence of the two modes produce different interactions within mesoscale systems and between the mesoscale and large-scale environment (Hartmann et al. 1984; Mapes and Houze 1993).

One of the major objectives of the National Aeronautics and Space Administration's (NASA) Tropical Rainfall Measuring Mission (TRMM) is to measure tropical rainfall using a spaceborne radar along with microwave, infrared, and visible radiometers and to provide vertical profiles of latent heating for use in validating large-scale atmospheric circulation models (Simpson et al. 1988; Tao et al. 1990; Tao et al. 1993). The mission includes a ground-based validation program utilizing meteorological Doppler radars, rain gauge networks, disdrometers, and vertical profilers at a number of tropical sites worldwide. The Doppler radar observations provide opportunities for estimating local divergence profiles, thus providing information on convective–stratiform heating (Mapes and Houze 1993). Disdrometers provide point measurements of the DSD, which aid in the determination of appropriate reflectivity–rainfall rate relations and in the interpretation of vertical profiler observations of reflectivity, Doppler velocity, and spectral width. Both the spaceborne and ground-based measurements will be used for precipitation classification and rainfall estimation. Thus, there is a need for improved understanding of the performance of classification algorithms and the physical processes that underpin their formulation.

According to the standard convective–stratiform definition, precipitation type can be identified in the presence of simultaneous observations of vertical air velocities and the terminal fall speed of hydrometeors (Houze 1993). Since, until very recently, these observations have been rare, indirect methods have been developed based on various observed properties of convective and stratiform clouds. For instance, the stratiform environment is horizontally more uniform than the convective. This feature is widely used to distinguish between the two types by scanning radar (e.g., Churchill and Houze 1984; Steiner et al. 1995), passive microwave (Kummerow et al. 1991), and infrared and visible (Adler and Negri 1988) satellite studies. In addition, a sharp increase in precipitation fall velocity near the melting level (Williams et al. 1995, WEG hereafter) and a well-marked radar ''bright band'' in stratiform rain can be used as criteria for discriminating between the precipitation types (Rosenfeld et al. 1995) as well as for validating the classification (Churchill and Houze 1984; Steiner et al. 1995).

In this study, the performance of two independent precipitation classification techniques developed for determining precipitation regimes in tropical cloud systems are intercompared and evaluated. Both methods have been applied to data collected during the Intensive Observing Period (IOP; November 1992–February 1993) of the Tropical Ocean Global Atmosphere Coupled Ocean–Atmosphere Response Experiment (TOGA COARE) at Kapingamarangi Atoll (near 1°N, 155°E). The first (TS) technique relies on characteristics of DSD parameters obtained from a surface-based disdrometer; the other technique, an extension of the WEG study, is based on the vertical structure of Doppler velocity and spectral width extracted from 915-MHz wind profiler observations. The disdrometer method classifies the precipitation type into two categories: 1) convective and 2) stratiform, while the profiler method has four categories: 1) shallow convective, 2) deep convective, 3) mixed convective–stratiform, and 4) stratiform.

The disdrometer algorithm was inspired by the study of Waldvogel (1974). By fitting observed DSDs to an

exponential distribution of the form $N(D) = N_0 \exp(-\Lambda D)$, and observing the variation of N_0 as well as the radar reflectivity profile, Waldvogel observed low values of N_0 associated with a bright band overhead in widespread rainfall without convective activity. He also noted that sudden increases of N_0 were correlated with the disappearance of the radar bright band, an indication of convective activity. In more recent work, Heinrich et al. (1996) have shown clear evidence of a relationship between riming processes (an indication of updrafts and convection), N_0, and the median volume diameter, D_0, of the raindrop spectra. Both N_0 and D_0 showed dramatic changes as riming increased, at times without changes in rain rate. In addition, the radar bright band was absent when strong riming was evident. The studies carried out by Waldvogel and his colleagues have focused on midlatitude orographic precipitation during winter. Tokay and Short (1996) proposed an empirical convective–stratiform classification method based on tropical DSD information. An extended description of their DSD based precipitation type algorithm can be found in TS.

Recently, a 915-MHz wind profiler system originally developed for observations of lower-tropospheric winds by the National Oceanic and Atmospheric Administration Aeronomy Laboratory was used to determine the structure of precipitating cloud systems in the Tropics (Gage et al. 1994; Ecklund et al. 1995). WEG developed a classification algorithm applied to 30-min average profiles of the Doppler velocity and spectral width observed on the vertical beam of the 915-MHz profiler located at Manus Island (2°S, 147°E). While the equivalent reflectivity is not used directly in the current profiler algorithm, it provides an important diagnostic for interpreting the results of the classification scheme. The precipitation types were distinguished based largely on the melting layer signature determined by the Doppler velocity gradient (DVG). The same algorithm was also applied to data from several other profilers located in the western tropical Pacific, for example, Christmas Island (2°N, 157°W; Gage et al. 1996). The rainfall at the surface was determined by tipping-bucket and optical rain gauges.

A brief description of the data and methods used here is given in sections 2 and 3, respectively. In section 4, general statistics of precipitation types are presented based on disdrometer, profiler, and joint disdrometer–profiler classification. Time–height sections of profiler products, that is, equivalent reflectivity, Doppler velocity, and spectral width, are investigated for the four case studies of TS in section 5. The characteristics of raindrop size distributions and of integral parameters is examined for each of the four profiler classifications in section 6; the mean equivalent reflectivity, Doppler velocity, and spectral width profiles based on profiler and disdrometer classifications are presented and intercompared in section 7. The results of this study are discussed in section 8, and the findings of the present study can be found in the conclusions.

2. Data

A total rainfall amount of 535 mm was recorded by the RD-69 Distromet disdrometer located at Kapingamarangi Atoll in 7605 rainy minutes during 105 days of the TOGA COARE IOP from 1 November 1992 to 13 February 1993. During the same time period a tipping-bucket gauge also located on the atoll recorded a total rainfall of 525 mm for the same events recorded by the disdrometer and an additional 320 mm of rainfall that occurred while the disdrometer was not recording data. One-minute rainfall rates were directly calculated from disdrometer DSDs (for rainfall rate > 0.1 mm h^{-1}).

Kapingamarangi Atoll also had a 915-MHz, ultrahigh frequency (UHF) wind profiler, which recorded Doppler spectra at 50 range gates. The UHF wind profiler considered here was developed for observing the lower tropical atmosphere. It is a small, low-powered device that can be operated unattended in almost any location, including remote areas such as atolls (Carter et al. 1995). Because of their wavelength (33 cm), these profilers are more sensitive to precipitation than other wind profilers that typically operate at longer wavelengths. The 915-MHz profilers operate in three different modes: low-height mode, high-height mode, and Radio Acoustic Sounding System (RASS) mode. In this study, the high-height mode, which samples the atmosphere up to 12.6 km with 225-m range gate spacing, was used with a dwell time of 30 s. The vertical profiles of radar reflectivity, Doppler velocity, and spectral width were extracted from the Doppler spectra of the vertically pointing beam about every 3 min. A detailed discussion of the characteristics of the 915-MHz profiler system and the processing of its data can be found in WEG.

3. Classification algorithms

Precipitation was classified as convective or stratiform by the disdrometer-based DSD. The separation between convective and stratiform precipitation was determined on the basis of a jump in the intercept parameter (N_0) of the gamma-fitted drop size distribution [$N(D) = N_0 D^m e^{-\Lambda D}$], following the physical arguments of Waldvogel (1974). It was found that $N_0 = 4 \times 10^9 R^{-4.3}$, where R is the rainfall rate and is a good threshold to distinguish between the two types of precipitation. In addition, $\Lambda = 17R^{-0.37}$, where Λ is the slope parameter of the gamma-fitted distribution, agrees well ($>$98%) with the N_0–R classification technique. It should be noted that third, fourth, and sixth moments of observed spectra (following Kozu and Nakamura 1991) were used in fitting the three-parameter gamma drop size distribution to the disdrometer observed raindrop spectra. More detailed information on the methodology of the drop size distribution based precipitation classification is given by TS. A flowchart of the disdrometer classification scheme is also given in Fig. 1.

The wind profiler algorithm presented in WEG was

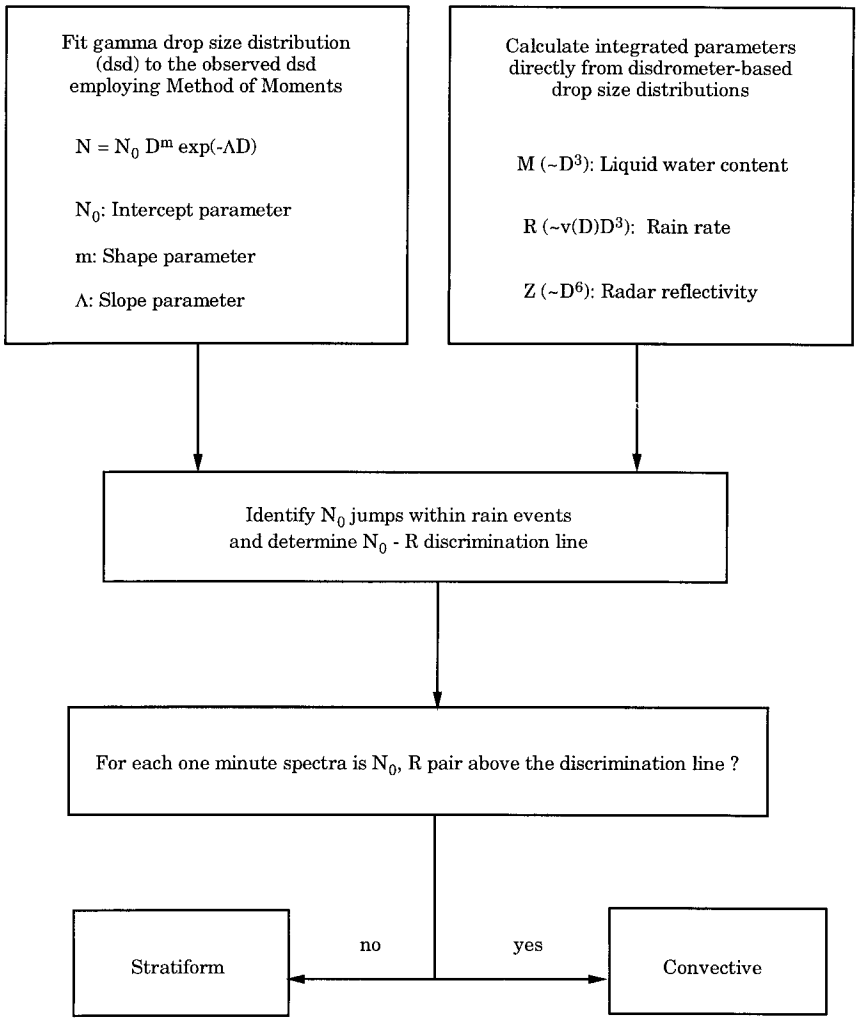

FIG. 1. A flowchart of the precipitation type algorithm developed by Tokay and Short (1996).

based on 30-min-averaged profiler observations that were coincident with precipitation recorded at the surface by a tipping-bucket rain gauge. The 30-min intervals containing at least one tip were classified as rainy, resulting in a minimum rainfall rate of 0.5 mm h^{-1}. In the present study, the same algorithmic approach is applied to 30-s samples of profiler observations with some minor modifications of thresholds that will be discussed later in the text.

The profiler algorithm determines four classes of precipitating clouds: stratiform, mixed stratiform–convective, deep convective, and shallow convective. The stratiform and mixed stratiform–convective classes were characterized by the presence of a melting layer signature identified by a change in hydrometeor fall speed associated with melting hydrometeors. The vertically pointing beam of the profiler measures the Doppler velocity, which is the sum of the fall speeds of the hydrometeors and vertical air velocity, and the DVG is sensitive to the microphysics associated with the melting layer. There is a strong correlation between increasing DVG and increasing brightband reflectivity. The threshold of DVG used for this study is 2 m s^{-1} km^{-1} applied between 3.5 and 5 km, and its sensitivity is tested over the interval from 2 to 4 m s^{-1} km^{-1}. A threshold of 2 m s^{-1} km^{-1} was applied by WEG to 30-min-averaged profiles, and the sensitivity was tested by varying the DVG between 1 and 3 m s^{-1} km^{-1}. The mixed stratiform–convective class was separated from the stratiform class by evidence of increased turbulent motion above the melting level, as indicated by spectral width. A spectral width above 7 km greater than 2.5 m s^{-1} was used by WEG as the threshold for distinguishing mixed cases from stratiform. A sensitivity study regarding the spectral width threshold can be found in WEG. In this study, a 2.0 m s^{-1} threshold for spectral width was adopted implying less turbulence above the melting level for the stratiform classification. The deep convective class had hydrometeor echoes above the melting level but did not have a melting layer signature, while shallow convec-

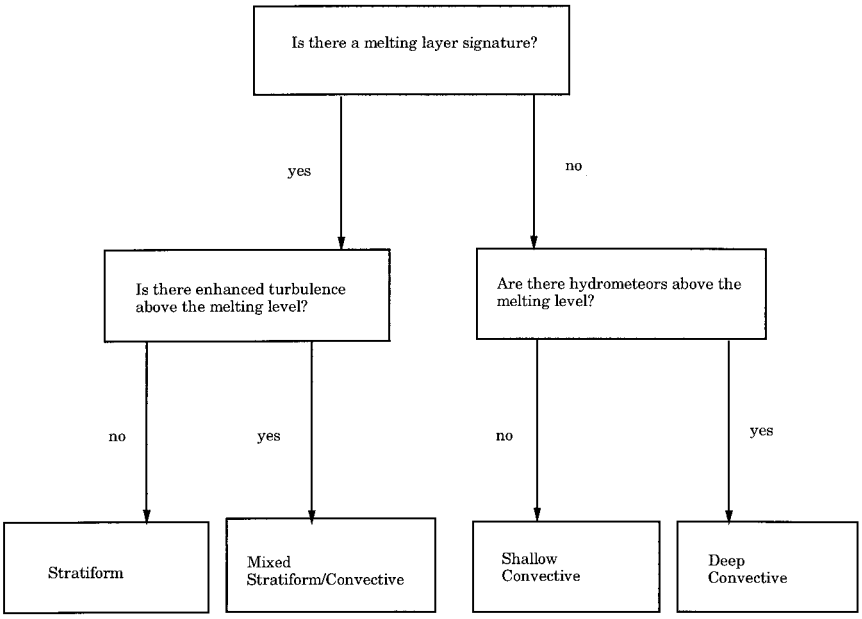

FIG. 2. A flowchart of the precipitation-type algorithm developed by Williams et al. (1995).

tion did not have hydrometeor echoes above the melting level. A Doppler velocity greater than 0.5 m s^{-1} at any altitude above 5 km was used by WEG to indicate the presence of deep clouds and thereby to discriminate between deep and shallow convective clouds. In this present study, the test height was raised to 7 km to avoid the influence of the melting level. More detailed information on the methodology of the wind profiler–based precipitation classification is given by WEG. A flowchart of the profiler classification scheme is given in Fig. 2.

4. Classification statistics

a. Disdrometer

During 105 days of the TOGA COARE IOP (1 November 1992–13 February 1993), the RD-69 Distromet disdrometer on Kapinagamarangi recorded 535 mm of rain during 7605 min. Using the classification technique described in TS, all 7605 min of data were divided into either stratiform or convective rain. Stratiform rain accounted for 74% occurrence but only 32% of total rainfall. This is consistent with previous studies in which the amount of surface rainfall from convective clouds exceeds that from stratiform clouds, while the reverse is true for the duration of surface rainfall (Steiner et al. 1995). As a result, the average rainfall rates were 11.0 and 1.8 mm h^{-1} for the convective and stratiform precipitation, respectively.

TABLE 1. Statistics of disdrometer classifications with simultaneous profiler observation.

	Disdrometer classification		
	Convective	Stratiform	Total
Number of samples (min)	417 (25%)	1273 (75%)	1690 (100%)
Rain accumulation (mm)	75 (64%)	42 (36%)	117 (100%)
Average rain rate (mm h^{-1})	10.51	1.86	4.15

As discussed in section 3, the data rates for the disdrometer and profiler are different with the disdrometer collecting data at one sample per minute and the profiler collecting one sample every 3 min. In addition, the profiler operated in a RASS mode for 5 min during every 30-min period. In order to compare the disdrometer observations with the profiler observations, only the disdrometer data with a rainfall rate greater than 0.1 mm h^{-1} and a profiler observation within a 1-min window were used in this study. This 1-min criteria produced a dataset consisting of 1690 simultaneous disdrometer and precipitating profiler observations. The statistics for this subset of disdrometer data are listed in Table 1. The subset had only a minor change with no bias in statistics from the complete disdrometer dataset.

As mentioned in the introduction, stratiform rain has larger horizontal spatial scales than convective rain. These large spatial scales are consistent with long temporal scales for single-point observations. Thus, stratiform rain events should have longer durations relative to convective rain events. The duration of the observed stratiform and convective precipitation events was determined by adding the number of consecutively classified minutes of rain identified in the 7605 min of disdrometer rain data. There was no attempt to interpolate over missing data or to remove or replace data when

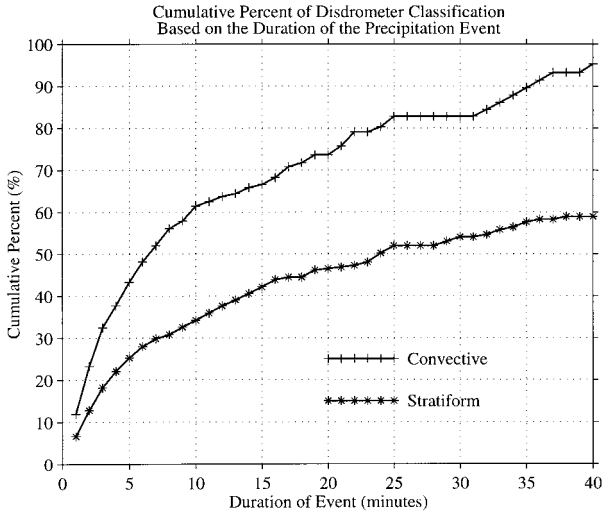

FIG. 3. Cumulative percent of disdrometer-classified stratiform and convective precipitation with duration less than the number of minutes specified on the abscissa.

the classification was questionable. The accumulated percent as a function of duration for both classes of precipitation events is shown in Fig. 3. The duration that corresponds to the 50% accumulated percent is where there are equal number of minutes in events shorter or longer than this 50% duration. The 50% duration for stratiform rain is 24 min and 7 min for convective rain. These median values are consistent with the conceptual model of tropical stratiform and convective rain.

Both of the techniques discussed in this paper classify precipitation type based on the characteristics of instantaneous observations. Neither technique uses the information from neighboring observations to support or modify a particular classification. The time persistence of stratiform rain events shown in Fig. 3 will be used in section 7 to help identify ''robust'' stratiform rain events.

b. Profiler

During the TOGA COARE IOP, the profiler recorded 39 773 vertical profiles in the high-height mode sampling the atmosphere from 0.25 to 12.5 km. The radar identified precipitation below 2 km in 6104 profiles (15%) and classified the profiles into the four classes shown in Table 2. The profiler observations that are within 1 min of a disdrometer observation compose the subset used for comparison with the disdrometer data. The statistics for this profiler subset are also listed in Table 2.

The statistics listed in Table 2 can be compared to the classification results reported by WEG in their Tables 2 and 3. The WEG results were obtained for Manus Island using 30-min-averaged profiler data. The present study employs instantaneous profiler observations from Kapingamarangi. Considering the fact that no systematic site-to-site variations of rainfall statistics occurs among the COARE integrated sounding system sites for the COARE IOP, any substantial disagreement in statistics between here and the WEG study can be attributed to the use of instantaneous versus 30-min-averaged profiles. The temporal averaging reduces the magnitude of the Doppler velocity gradient and therefore reduces the number and duration of events classified as stratiform precipitation. The use of the same DVG threshold for the instantaneous dataset will then increase the number and duration of events classified as stratiform precipitation. In that respect, it is not surprising that the present study reveals higher percentages of stratiform rain in both amount and duration than the WEG study.

Direct comparison between the profiler and disdrometer classifications for the 1690 observations is shown in Table 3. Considering the differences between WEG and current rainfall statistics due to the use of averaged versus instantaneous samples, the results in Table 4 show reasonable agreement. The stratiform class was identified by both techniques for 820 profiles or for 65% of the disdrometer stratiform classifications. The remaining 35% of the disdrometer stratiform classifications occur mostly in the profiler's mixed category (24%), with 11% divided between the deep and shallow convective categories. The disdrometer convective classification is widely distributed among the four profiler categories with 30% classified as convective, while one-third of precipitation falls in the stratiform category. However, the average rainfall rate for these 138 profiler stratiform samples is 12.61 mm h^{-1}, which is more consistent with convective rainfall.

It is important to recognize the inherent difficulties in comparing the classification inferences from surface measurements with classification inferences from vertical structure observations primarily in the 4–7-km

TABLE 2. Statistics of profiler classifications with simultaneous disdrometer observations.

	Profiler classification				
	Shallow convective	Deep convective	Mixed stratiform–convective	Stratiform	Total
Number of profiles	125 (7%)	152 (9%)	455 (27%)	958 (57%)	1690 (100%)
Rain accumulation (mm)	7 (6%)	13 (11%)	44 (38%)	53 (45%)	117 (100%)
Average rain rate (mm h^{-1})	3.36	5.13	5.80	3.32	4.15

TABLE 3. Statistics of joint disdrometer–profiler classifications.

	Profiler classification				
	Shallow convective	Deep convective	Mixed stratiform–convective	Stratiform	Total
Number of profiles					
Disdrometer convective	56 (13%)	70 (17%)	153 (37%)	138 (33%)	417 (100%)
Disdrometer stratiform	69 (5%)	82 (6%)	302 (24%)	820 (65%)	1273 (100%)
Rain accumulation (mm)					
Disdrometer convective	5 (7%)	10 (13%)	31 (41%)	29 (39%)	75 (100%)
Disdrometer stratiform	2 (5%)	3 (7%)	13 (31%)	24 (57%)	42 (100%)
Average rain rate (mm h^{-1})					
Disdrometer convective	5.36	8.57	2.16	12.61	10.79
Disdrometer stratiform	1.74	2.20	2.58	1.76	1.98

range. Fundamentally, there is a time–space ambiguity introduced by the fact that it typically takes 15 min or longer for hydrometeors at the melting level to reach the surface. Obviously, under realistic wind conditions, profiler observations recorded instantaneously from the same location as the disdrometer would be best compared with surface measurements taken *downstream* where the hydrometeors are actually impacting the surface. Conversely, disdrometer observations recorded instantaneously at the surface would be best compared to profiler observations taken earlier *upstream*.

The determination of the DVG threshold is crucial for the profiler algorithm and therefore plays an important role in the intercomparison of the precipitation classifications. The sensitivity of the DVG threshold to the identification of precipitation type indicates that disdrometer and profiler algorithms are in best agreement when the DVG threshold is 3.5 m s^{-1} km^{-1}, as shown in Table 4. In this intercomparison, the the output of the profiler algorithm is reduced to convective and stratiform categories. The mixed category is considered first as stratiform and then as convective. The agreement in rain totals shows a substantial increase as the DVG threshold increases from 2 to 3.5 m s^{-1} km^{-1}, regardless of the determination of the mixed category as either stratiform or convective. At the same time, the agreement in number of samples decreases only a few percent for the same increment. This implies that the DVG threshold used in the WEG study is somewhat small for the current study.

TABLE 4. The sensitivity of DVG threshold to the precipitation type. Agreement between profiler and disdrometer classification when the mixed profiler classification is considered as stratiform and as convective (values in parenthesis).

DGV (m s^{-1} km^{-1})	Agreement in rain totals (%)	Agreement in rain events (%)
>2.0	44 (65)	74 (60)
>2.5	54 (65)	74 (66)
>3.0	61 (64)	73 (69)
>3.5	72 (63)	71 (74)
>4.0	73 (59)	67 (73)

More discussion about the similarities and differences between the disdrometer and profiler classification will be presented in the next three sections. In the next section, several case studies are examined to show the evolution of the vertical structure observed by the profiler above the surface disdrometer measurements. In the following section, the vertical structure observations of the profiler are used diagnostically to gain further insight into the cause of some of the discrepancies seen in Tables 2 and 3.

5. Case studies

Tokay and Short (1996) analyzed 15 major rain events and presented 4 of them in their paper. Here the same four events are reexamined including the time–height sections of equivalent reflectivity, Doppler velocity, and spectral width derived from profiler observations. The original disdrometer and profiler observations are shown in their respective 1- and 3-min data rates. In this section we present four case studies for the following periods: (a) 19 December 1992, (b) 26 January 1993, and (c) 5 February 1993. For each event we illustrate the vertical structure and the detailed classification results for both disdrometer and profiler.

a. 19 December 1992

The first event has about 11 h of continuous rain (Fig. 4). The disdrometer-determined convective classification was dominant, indicating light showers until 0700 UTC, followed by 3 h of heavy showers, followed by 4 h of rain with a predominant stratiform classification. The profiler shows a well-defined DVG and bright band (BB) between 1000 and 1400 UTC, during the stratiform rain observed at the surface. The profiler classifies deep convective, mixed, and stratiform clouds with the presence of a small DVG and a narrow zone of large variations in Doppler spectra between 0400 and 0530 UTC

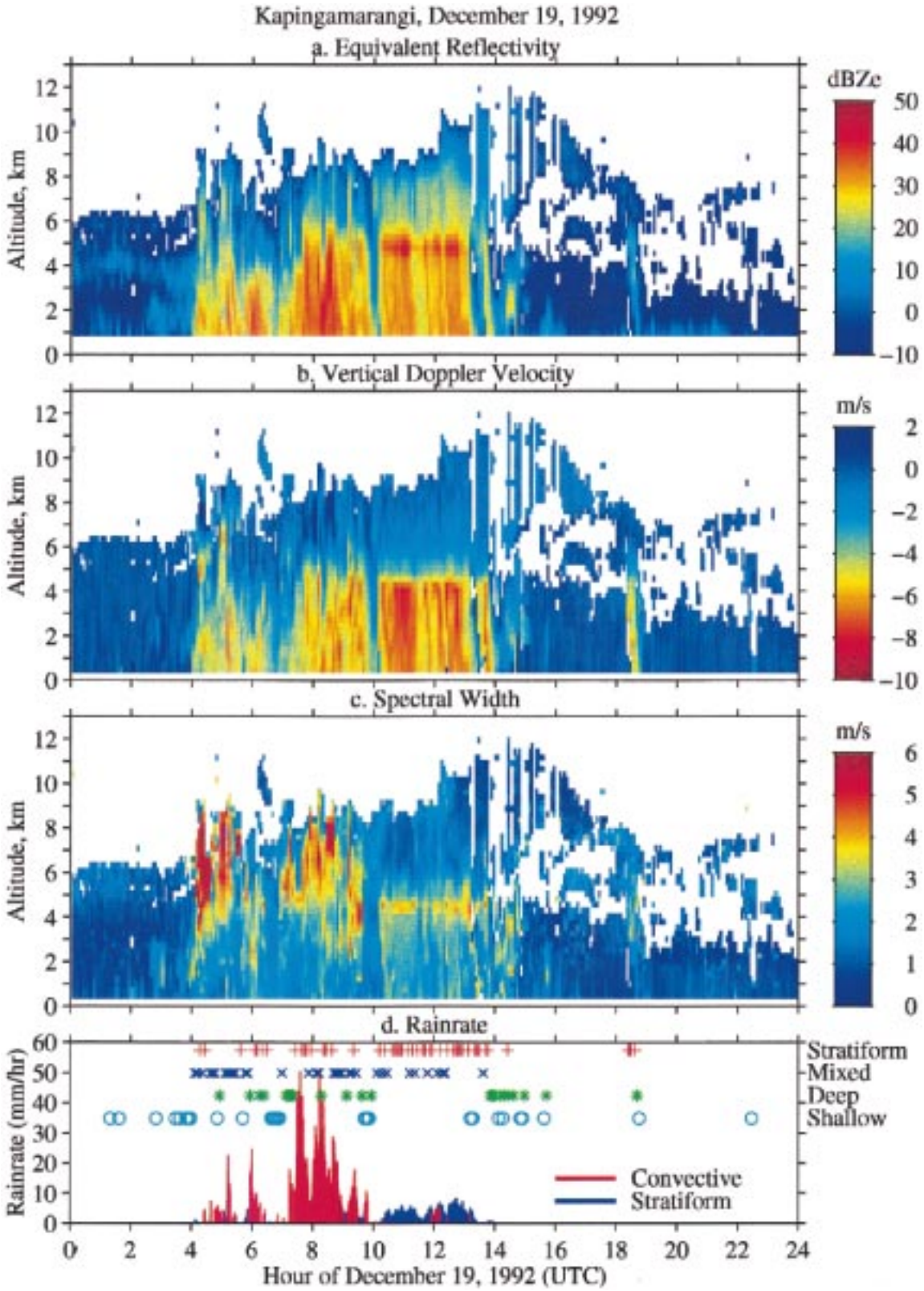

FIG. 4. A case study for 19 December 1992 (nighttime). Time–height cross section of (a) equivalent reflectivity, (b) Doppler velocity, (c) spectral width, and (d) 1-min rain rate from convective (red) and stratiform (blue) clouds as classified by the disdrometer. The precipitation type identified by the profiler classification is also given in (d).

during light showers at the surface. However, no signature of a BB is observed for this 1.5-h period. The peak reflectivities are below the BB region (less than 4 km). The rain-rate time series also shows substantial variations in rain rate in short time periods as one of the characteristics of convective rain. Under these conditions the profiler-determined mixed and stratiform regimes in light showers should be regarded as convective as well. During heavy showers, the profiler had two classifications: deep convective and mixed (convective–stratiform). The mixed regime again resulted from a small DVG and variations in Doppler spectra at 5–8 km. Reflectivities above 35 dB*Z* located below the BB altitude are present between 0745 and 0845 UTC. The mixed regime is clearly convective from the reflectivity profile as well as rain rates exceeding 20 to 40 mm h^{-1}. This event illustrates the fact that the profiler algorithm used here does not differentiate effectively convective from stratiform precipitation in the presence of a small DVG. Also there are examples of misclassification by the disdrometer that occasionally indicate stratiform precipitation during convective conditions.

b. 26 January 1993

There were two rain events on 26 January 1993 that we examine here. Two hours of predominantly convective rain during midday on 26 January 1993 was followed by nighttime showers (Fig. 5). There is no BB signature during the first rain event. However, a small DVG results in a brief period of stratiform classification as diagnosed by the profiler and the disdrometer at times also indicates unsteady stratiform classifications. A nonuniform structure in the rain-rate time series with rain rates exceeding 20 to 30 mm h^{-1} indicates that convective rain is predominant.

The second rain event on 26 January 1993 (the third case), has 2 h of disdrometer-classified convective rain followed by over 4 h of disdrometer-classified stratiform rain. The profiler shows the presence of hydrometeors extending to 6 km or higher levels, indicating deep convective, mixed convective–stratiform, and stratiform clouds. A large DVG and a well-developed brightband signature are present between 1400 and 1800 UTC during the disdrometer-classified stratiform rain at the surface. The echo tops extend above 12 km between 1400 and 1600 UTC with spectral widths of 3–5 m s^{-1} at around 12 km. The mixed regime in this period is probably stratiform. The first hour of convective rain is associated with developing echo tops, a small DVG, reflectivities above 40 dB*Z* near 2 km, and large spectral width between 2 and 7 km. The mixed regime due to a small DVG and spectral widths of 3–4 m s^{-1} above 7 km is convective in this case. The stratiform regime in the profiler classification is due to a small DVG during the second hour of disdrometer-classified convective rain at the surface, representing the transition regime and a possible time lag between the two classifications. A 15–30-min lag between the two classification algorithms improves the agreement considerably for this case.

c. 5 February 1993

The fourth case is a short event (Fig. 6) comprised of 3 h of light rain. The disdrometer classification suggests convective rain until 1100 UTC followed by stratiform rain for the last 2 h of the event. Most of the rain is confined to rates between 1 and 10 mm h^{-1} where both convective and stratiform rain frequently occur; therefore, the performance of each algorithm is more crucial in identifying the precipitation type. The profiler has a well-defined DVG and a BB between 1130 and 1300 UTC during the stratiform rain at the surface. Variations in the spectral width are generally weak except at 1015 UTC above 10 km. The profiler classifies mixed and stratiform regimes for the entire event. The DVG is relatively weak at the earlier stage and the rain rates show jumps exceeding 10 mm h^{-1}, suggesting a convective nature for the event. Following 1100 UTC the profiler classification of mixed is based on a high-level increase of spectral width around 10 km that is not connected with the surface precipitation. Indeed, the minimum values of spectral width above 6 km after 1100 UTC indicate that stratiform precipitation is the appropriate classification. However, before 1100 UTC the mixed regime classified by the profiler has characteristics that may be more attributable to convective precipitation.

While the mixed convective–stratiform regime of the profiler can often be attributed to either convective or stratiform precipitation regimes based on echo characteristics, the hour before 1100 UTC on 5 February provides an example where a third classification may be useful. In other cases profiles with averaged reflectivities larger than 35 dB*Z*, no brightband signature, and only a small DVG may be more appropriately classified as convective rain. In addition, the echo tops gradually increase in convective rain, while relatively less variations are expected in stratiform rain. A small DVG can result from the presence of graupel particles, observed with a bright region in the reflectivity profile in convective rain. In some cases, a small DVG may not be associated with any bright region. A large variation in spectral width at a few levels may not be sufficient for classifying the mixed regime. At the same time, short jumps between disdrometer-classified convective and stratiform rain within the rain-rate time series can be clarified by examining the vertical structure evident in the profiler observations. A nonuniform structure in the rain-rate time series with values exceeding 10 mm h^{-1} can be another indication of convective rain.

The case studies presented here show the evolution of the vertical structure of precipitating clouds over the disdrometer and offer an explanation for the existence of relatively high rain rates in the profiler mixed con-

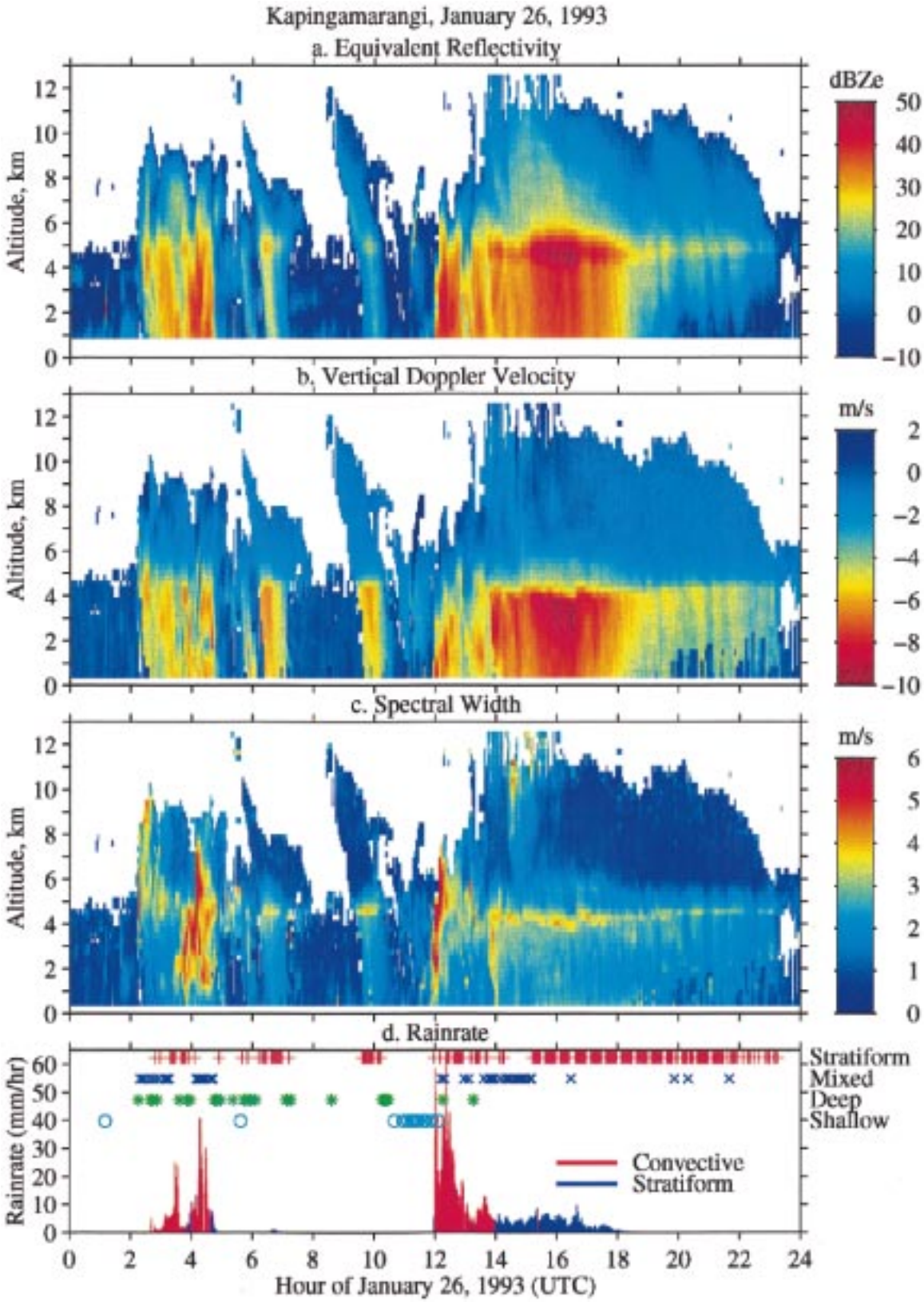

FIG. 5. A case study for two rain events on 26 January 1993 (daytime and nighttime). Time–height cross section of (a) equivalent reflectivity, (b) Doppler velocity, (c) spectral width, and (d) 1-min rain rate from convective (red) and stratiform (blue) clouds as classified by the disdrometer. The precipitation type identified by the profiler classification is also given in (d).

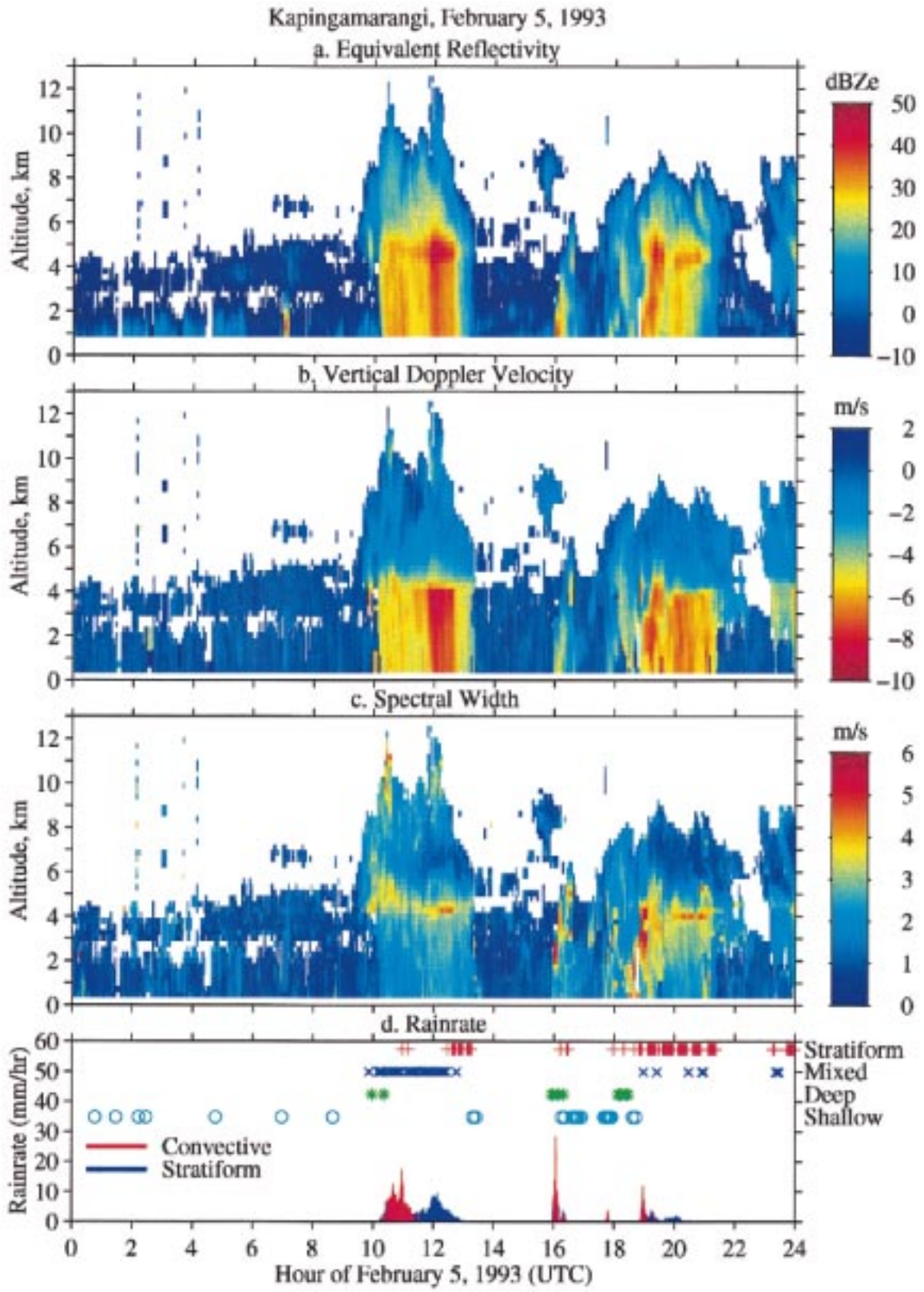

FIG. 6. A case study for 5 February 1993 (nighttime). Time–height cross section of (a) equivalent reflectivity, (b) Doppler velocity, (c) spectral width, and (d) 1-min rain rate from convective (red) and stratiform (blue) clouds as classified by the disdrometer. The precipitation type identified by the profiler classification is also given in (d).

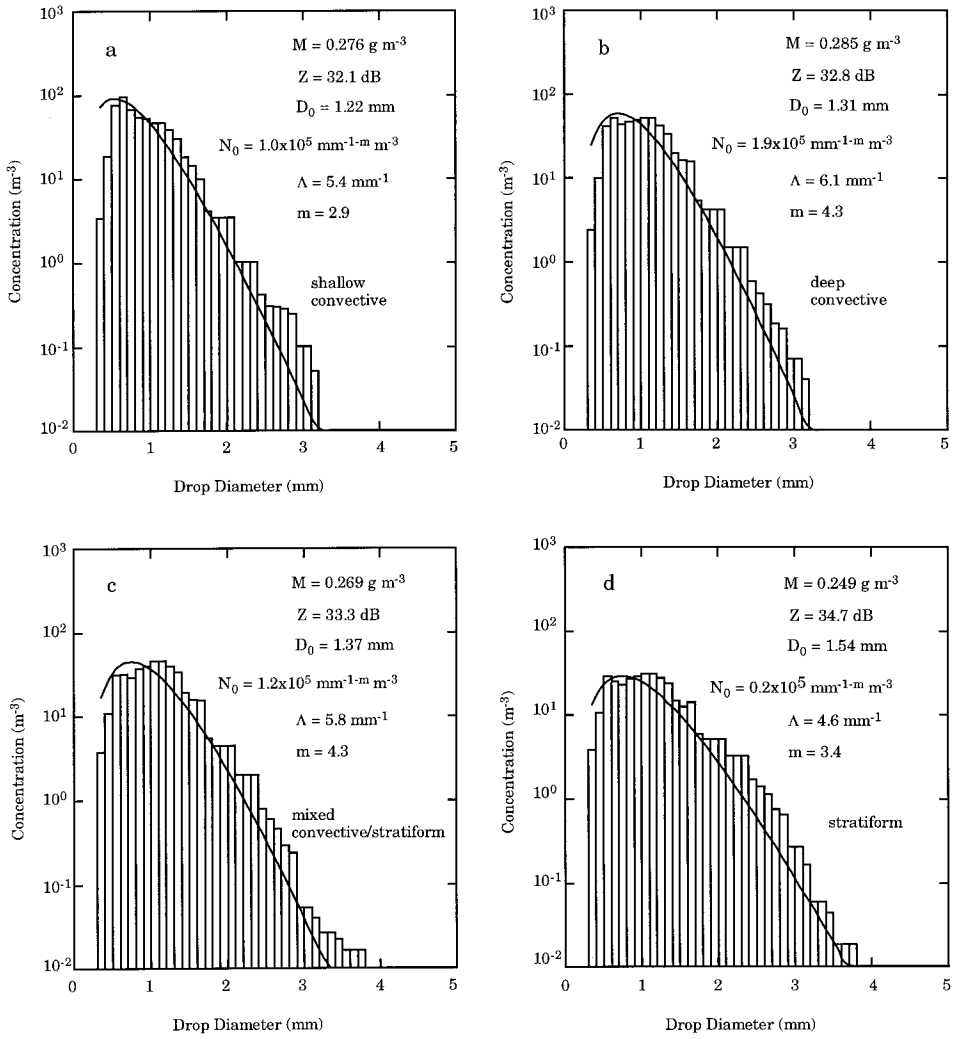

FIG. 7. Observed and fitted composite spectra for the profiler's (a) shallow convective, (b) deep convective, (c) mixed stratiform–convective, and (d) stratiform rain from 6, 21, 115, and 106 spectra, respectively, for rainfall rates of 5 mm h^{-1}.

vective–stratiform classification. The small DVG together with spectral width enhancements above the freezing level results in mixed convective–stratiform classifications during heavy rain episodes, as shown in most of the cases. In some cases, a small DVG alone was sufficient for stratiform classification during heavy rain showers.

6. Raindrop size distribution in relation to disdrometer and profiler-based classification of tropical precipitation

Convective and stratiform occurrences, as determined by the disdrometer algorithm, are almost evenly divided when the rain rate is between 1 and 10 mm h^{-1}. This is the range where distinctions between rain types may be more difficult to evaluate. Tokay and Short (1996) examined the averaged raindrop spectra (gamma and integral parameters) of convective and stratiform regimes in a narrow window of rain rates around 5 mm h^{-1} (Fig. 6 in TS). The liquid water content M decreased by 0.047 g m^{-3}, while the mean volume diameter D_0 and the radar reflectivity Z increased by 0.37 mm and 3.7 dBZ from convective to stratiform spectra, respectively.

The individual DSDs, having rain rates between 4.5 and 5.5 mm h^{-1}, were averaged for the four different profiler's precipitation classifications and the best-fit estimates were determined by the method of moments (Fig. 7). The composite spectra include 6 shallow convective, 21 deep convective, 115 mixed stratiform–convective, and 106 stratiform cases.

The characteristics of raindrop spectra and integral parameters agree well with those found in the TS study. For example, the composite spectra of deep convective rain is narrower than that of stratiform rain. This is

consistent with the TS observations that at the same rain rate, fewer large drops are found in convective rain than in stratiform. Therefore, M decreases by 0.043 g m^{-3}, while D_0 and Z increase by 0.29 mm and 2.1 dBZ, respectively, from deep convective to stratiform spectra. With respect to mixed spectra, the integral parameters have characteristics closer to deep convective spectra than to stratiform spectra. For instance, the difference in reflectivity is 0.6 dBZ between deep convective and mixed cases, while a 1.5 dBZ difference is present between mixed and stratiform cases. The size distribution for shallow convective rain (Fig. 7a) is relatively narrow with a maximum drop diameter of 2.5 mm. The spectra are consistent with the observations taken in Hawaiian showers (Beard and Tokay 1991).

7. Vertical structure of equivalent reflectivity, Doppler velocity, and spectral width in relation to disdrometer and profiler-based classification of tropical precipitation

One can construct 14 different types of vertical profiles of mean equivalent reflectivity, Doppler velocity, and spectral width for intercomparison of the two classification methods. In this section we compare vertical profiles based on the two disdrometer, four profiler classifications, and eight different permutations of the two methods. The mean profiles are constructed by averaging profiler reflectivities, Doppler velocities, and spectral widths at each height when the disdrometer recorded rainfall at the surface. Note that the first three gates of the reflectivity profile and the first gate of the Doppler velocity and spectral width profiles are not plotted because of instrument recovery.

a. Disdrometer classifications

Vertical profiles of mean equivalent reflectivities are contained in Fig. 8a for the stratiform and convective disdrometer classifications. The two disdrometer classifications exhibit a similar reflectivity profile above about 8 km. Just above the melting level (5–8 km) the convective reflectivities are systematically lower than the stratiform reflectivities. While there is a well-defined BB between 4- and 5-km altitude for the stratiform profile, there is no BB present in the convective profile. The BB in the stratiform profile is mostly confined between 4.4 and 4.7 km. The reflectivities for the stratiform classification are almost height independent below the brightband signature. A moderate increase in equivalent reflectivity is evident in the convective profile below 4 km, where the mean convective reflectivity exceeds that for the stratiform classification.

Doppler velocity profiles for the two disdrometer classifications are shown in Fig 8b. Generally, these two profiles look very similar especially above the melting level. At the melting level, Doppler velocities for both classifications become more negative downward and

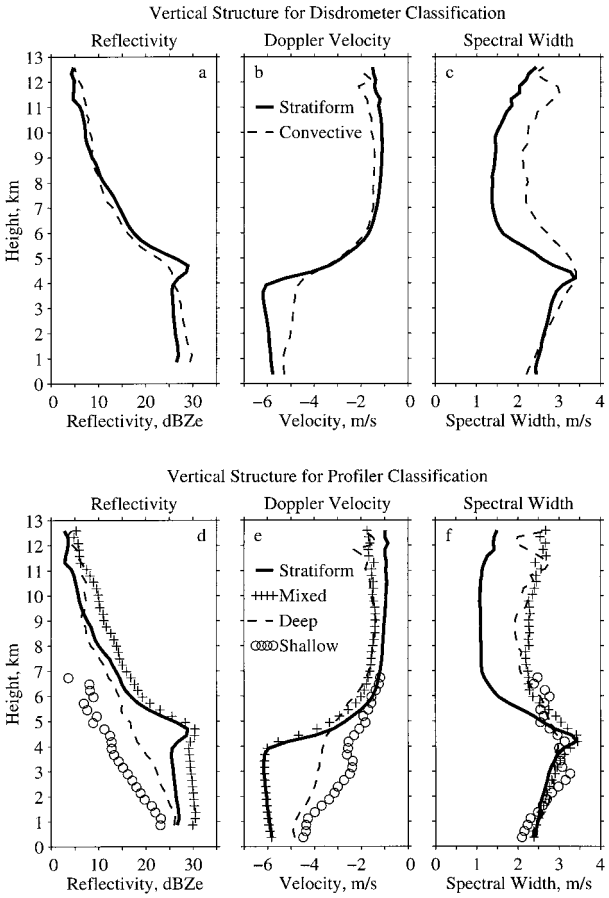

FIG. 8. Vertical structure for disdrometer classification (top) and for profiler classification (bottom). The top panel contains profiles of (a) mean equivalent reflectivity, (b) Doppler velocity, and (c) spectral width for stratiform and convective disdrometer classifications. The bottom panel contains profiles of (a) mean equivalent reflectivity; (b) Doppler velocity; and (c) spectral width for stratiform, deep convective, mixed, and shallow profiler classifications.

track one another until about 4.5 km, where the stratiform profile becomes more negative than the convective profile. Below 4 km the Doppler velocity in the stratiform profile is more negative at all altitudes compared to the convective profile. In addition the vertical gradient of Doppler velocity below 4 km is opposite for the two classifications, suggestive of the effects of air density and evaporation on the stratiform size distribution and coalescence growth on the convective size distribution.

The fact that the disdrometer-determined convective profile shows a considerable DVG at the melting level implies the DVG criteria used by the profiler classification need to be examined carefully in terms of its ability to differentiate between convective and stratiform precipitation. Vertical profiles of spectral width for the two disdrometer classifications are shown in Fig. 8c. While the profiles are similar below the melting level, the spectral width is substantially larger for con-

vective precipitation above the melting level. This result is consistent with the expectation that stratiform conditions show only small vertical motions above the melting level.

b. Profiler classifications

The vertical structure for the four profiler classifications is shown in Figs. 8d–f. Reflectivity profiles for the four profiler classifications are shown in Fig. 8d. Comparison of the four profiles shows that the stratiform and deep convective classifications are less similar than for the disdrometer classifications. While the stratiform reflectivity profile is very similar to the stratiform disdrometer reflectivity profile, the deep convective profile has considerably less reflectivity than the disdrometer convective profile. For the mixed (stratiform–convective) profiler classification, the equivalent reflectivity exceeds the equivalent reflectivity for the convective and stratiform classifications at all levels. Although the mixed category shows little evidence of a BB, there is a fairly uniform reflectivity distribution with altitude below the melting level similar to the stratiform category. In contrast, the lowest reflectivities are evident for the shallow convection category. Both the shallow and deep convection profiler categories show substantial gradients in reflectivity with equivalent reflectivity increasing downward.

Above the melting level, the Doppler velocities (Fig. 8e) of the four profiler classifications are very similar except that the stratiform Doppler velocities are systematically weaker than for the deep and mixed categories. Below the melting level, the mixed profiler category shows a very similar profile to the stratiform category, while the deep and shallow categories have greatly reduced (less negative) vertical Doppler velocities. The stratiform Doppler velocity profile is very similar to the disdrometer-based stratiform profile but, as was the case for reflectivity, the deep convective Doppler velocity profile is more dissimilar to the stratiform profile than the disdrometer-based convective profile is to the disdrometer-based stratiform profile. In other words, the deep convective profile has substantially reduced Doppler velocities compared to the disdrometer-based convective profile.

As described above, mean Doppler velocity profiles of stratiform precipitation in Figs. 8b,e show a slight downward increase above 6 km followed by a rapid increase just above the melting level between 6- and 4-km altitude and a decrease below 4 km. The slight increase in mean Doppler velocity from 0.5 to 1.5 m s^{-1} at levels colder than -5°C is attributed to increases in the mass of ice crystals mainly due to vapor deposition. The increased fall velocity of aggregates is indicated by a rapid increase in Doppler velocity at around 6 km. A further increase in Doppler velocity is evident as a result of phase transitions at and below the melting level. The increase in Doppler velocity between 6 and 4 km is from 1.5 to 6 m s^{-1} in the mean profile. A decrease in Doppler velocity below 4 km is partially due to the atmospheric density effect on terminal velocities of raindrops such that raindrops fall faster aloft than near the surface, as indicated in WEG. In addition, the size distribution of raindrops is continuously modified as a result of microphysical processes, namely, evaporation and collision–coalescence.

Mean Doppler velocity profiles of convective precipitation in Figs. 8b,e show little variation above 8 km followed by a monotonic downward increase between 8 km and the surface. In contrast to stratiform clouds, vertical air motions are a significant component of the observed Doppler velocities. Therefore, the vertical variation of the Doppler velocity cannot be solely linked to the terminal fall speeds of hydrometeors. In the presence of strong updrafts, water droplets can penetrate to the upper and colder portions of the convective clouds where accretion by ice crystals leads to the formation of graupel. Typically, graupel hydrometeors have terminal velocities of 1.5 to 3.0 m s^{-1}, depending on their size, and fall faster than aggregate ice crystals found in stratiform clouds. The increase in observed Doppler velocities at and above the melting level may be due to the combined effects of the presence of graupel particles and the phase transition leading to the formation of liquid droplets. However, a sharp increase in Doppler velocity is not evident because of the upward air velocities.

Spectral width profiles are contained in Figs. 8c,f. The stratiform profile is very similar to the stratiform disdrometer profile, whereas the deep, mixed, and shallow categories are very similar to one another and similar to the convective disdrometer result. It is interesting to note from the above that the ''deep'' profiler classification seems to provide a clearer differentiation from stratiform conditions than the disdrometer ''convective'' category does. On the other hand, the DVG criteria by itself may not provide enough information to differentiate between convective and stratiform conditions.

c. Joint disdrometer–profiler classifications

The vertical structure associated with joint disdrometer–profiler classifications is illustrated in Fig. 9. Given a disdrometer-based classification of stratiform, the reflectivity profiles for the four profiler classifications are shown in Fig. 9a. When the disdrometer and profiler both indicate stratiform precipitation, the reflectivity profile is very similar to what is found when either the disdrometer or profiler alone indicate stratiform precipitation (cf. Fig. 8). Considering the fact that almost 90% of the disdrometer's stratiform classification satisfies the profiler's DVG criteria as indicated in Table 3, the mixed convective–stratiform and stratiform reflectivity profiles of profiler classification alone (cf. Fig. 8d) and of joint disdrometer–profiler classification (Fig. 9a) are quite similar to each other. The same is true for the Doppler velocity (Fig. 9b) and spectral width (Fig. 9c). A 90%

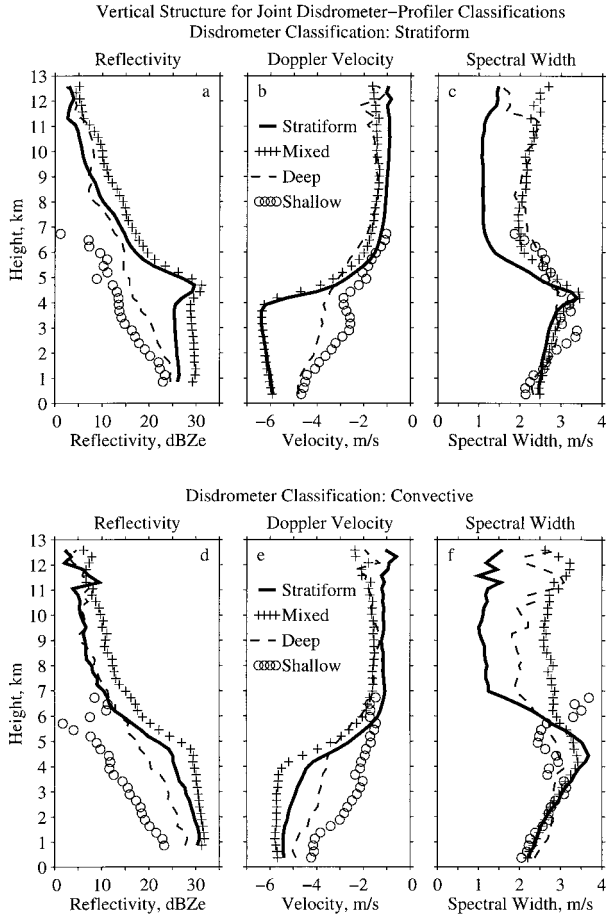

FIG. 9. Vertical structure for joint disdrometer–profiler classification. The top panel contains the profiles of (a) mean equivalent reflectivity, (b) Doppler velocity, and (c) spectral width for stratiform disdrometer classifications for each of the four profiler classifications. The bottom panel contains profiles of (d) mean equivalent reflectivity, (e) Doppler velocity, and (f) spectral width for convective disdrometer classifications for each of the four profiler classifications.

agreement suggests that given the disdrometer classification of stratiform precipitation, the joint disdrometer–profiler classification can be considered almost a subset of the profiler classification.

The vertical structure associated with the four profiler classifications, given that the disdrometer classifies the precipitation as convective, is illustrated in the bottom panel of Fig. 9. Unlike the results for the disdrometer-based stratiform classification, the convective classification by the disdrometer does influence the vertical structure of each of the four profiler categories. Under conditions that the disdrometer identifies as convective, the profiler-based stratiform reflectivity profile loses its BB, becomes weaker above the melting level, and stronger below the melting level. Most importantly, below the melting level when the disdrometer classifies the precipitation as convective, the profiler-based strafiform reflectivity profile shows increasing reflectivity between the melting level and the surface, as can be seen for other convective profiles. Compared to the profiler stratiform category, the profiler mixed category shows little change in structure when the disdrometer classifies the precipitation as convective. However, the change that is seen in the mixed category is in the same direction as for the stratiform category, that is, the reflectivity tends to decrease above the melting level, the BB disappears, and the reflectivity shows a slight increase with decreasing altitude below the melting level. The profiler-determined deep and shallow convective profiles, on the other hand, change very little when the disdrometer classifies the precipitation as convective.

The profiler-determined Doppler velocity profiles (Fig. 9e) change in a similar fashion when the disdrometer classifies the precipitation as convective. The greatest change, as for the reflectivity profile, is in the stratiform category, while only minor changes are seen in the shallow and deep convective categories. The stratiform profile shows reduced (downward) vertical Doppler velocities, showing a vertical structure more similar to the deep convective profile. The mixed category shows only a slight reduction in Doppler velocity.

The effect of the convective disdrometer classification on the vertical structure of spectral width for the four profiler categories can be seen by comparing Fig. 9f with Fig. 8f. Above 7 km and below 3 km the stratiform spectral width profile is changed very little. However, around the melting level the spectral width increases substantially. Again, as noted for reflectivity and Doppler velocity, the deep and shallow categories do not change very much when the disdrometer classifies the precipitation as convective. The mixed category, however, shows an increased spectral width above the melting level. The pronounced increase in spectral width implies the convective nature of the profile.

In summary, in this section the mean vertical profiles of equivalent reflectivity, Doppler velocity, and spectral width for disdrometer and profiler classifications and eight possible permutations of the two sets of classifications were examined to identify strengths, weaknesses, and synergies. The presence of a well-defined bright band when both algorithms classify as stratiform, and its absence when both algorithms classify as convective, shows consistency between the two algorithms. However, some disagreements arising mainly from the application of an algorithm tuned to 30-min-averaged profiles to instantaneous data are also evident. For example, the existence of a substantial number of profiler-based stratiform cases that approach the vertical structure of the deep convective cases when the disdrometer classifies convective precipitation implies that the profiler classification algorithm missclassifies some convective cases as stratiform, as noted in section 5.

8. Discussion

In section 4, basic statistics on the precipitation types from two independent classification methods were pre-

sented in terms of percentage of occurrence and of rainfall accumulation. In section 5, case studies provided further evidence of the temporal variability of classifications, the general agreement between the two methods, and possible reasons for differences between the two algorithms. In section 6, the characteristics of composite raindrop spectra at rain rates of around 5 mm h^{-1} constructed for the four different profiler classifications were examined. In section 7, we presented the average vertical structure seen by the profiler, which provided further insight into the fidelity of the two classification methods. Here, we review our findings and try to find an answer to the following questions. What is the reliability of profiler and disdrometer classifications of stratiform precipitation? What is the reliability of profiler and disdrometer classifications of convective precipitation? Is there a third category of precipitation?

The influence of the temporal persistence of the classification provided by the disdrometer will be considered first. Then the influence of the rainfall intensity on the classification of precipitation will be examined and, finally, the profiler mixed category will be examined as a third category of precipitation intermediate to convective and stratiform precipitation.

The joint distribution of disdrometer and profiler classifications contains examples when the same events are classified differently by both methods. Indeed, note that the disdrometer stratiform classification contains at times convective precipitation of the deep or shallow type (cf. Figs. 9d–f). Here we examine the influence of duration of disdrometer classification on the robustness of the stratiform classification. To illustrate the influence of the persistence of the classification, we show in Fig. 10 the vertical profiles of mean equivalent reflectivity, mean Doppler velocity, and mean spectral width for the stratiform disdrometer category when the stratiform classification persists for at least 20 min and when it is shorter than 5 min. The vertical profile of mean equivalent reflectivity for profiler-determined classifications for these two subclasses of stratiform disdrometer classification can be compared in Figs. 10a,d. It is immediately apparent that when the disdrometer stratiform classification is robust (i.e., persists for longer than 20 min) the reflectivity profiles for both profiler-determined stratiform and mixed categories have pronounced BBs. No cases of shallow convection and only three cases of deep convection are contained within the sample of robust disdrometer stratiform classification. Furthermore, this robust category of disdrometer stratiform classification contains 370 samples identified as stratiform by the profiler and 110 samples identified as mixed by the profiler. Examination of the mean Doppler velocity profiles in Fig. 10b and the spectral width profiles in Fig. 10c for the stratiform and mixed cases confirms that these profiler cases look very much like the stratiform cases in Figs. 8d–f. Only the mixed spectral width above the melting layer departs from this picture.

Restricting the disdrometer stratiform classification to those cases that have less than 5-min duration shows a different result. With the disdrometer stratiform classification in transition (nonrobust) the profiler classifies 53 samples as deep convection and 51 samples as shallow convection. Moreover, the 187 profiler-determined stratiform samples that fit into this category show a weaker reflectivity and much less pronounced BB. Indeed, the 83 mixed samples show no BB. The Doppler velocities for both profiler-determined stratiform and mixed categories also look less like the stratiform profiles in the top panel. The results of the analysis of persistence show that some of the shorter duration ''stratiform'' events classified by the disdrometer should more appropriately be classified as ''convective.'' Some of these misclassifications are undoubtedly due to the space–time ambiguity mentioned earlier. But some of the convective and stratiform classifications are really indeterminate as evidenced by their vacillation between

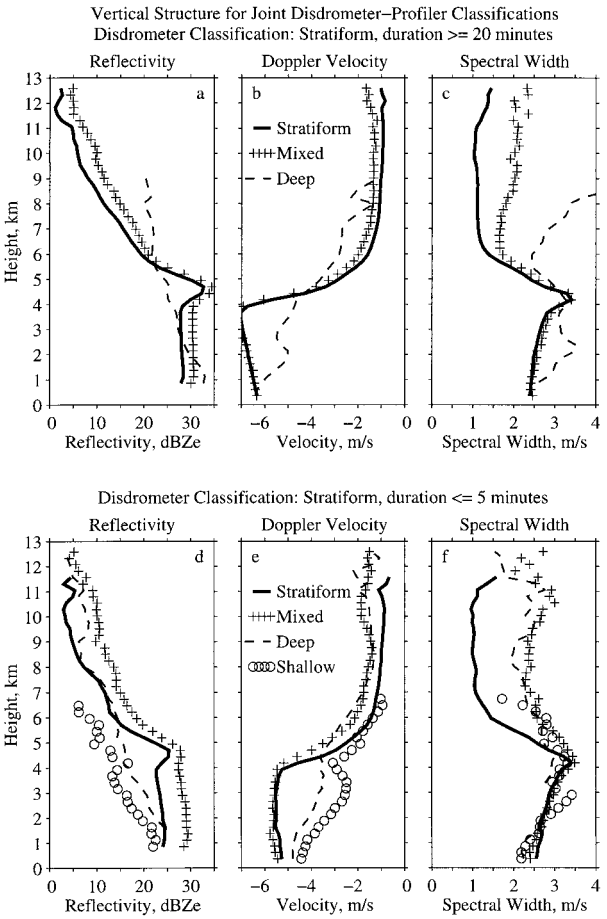

FIG. 10. Vertical structure for joint disdrometer–profiler classifications as a function of the duration of disdrometer stratiform classification. The top panel contains profiles of (a) mean equivalent reflectivity, (b) Doppler velocity, and (c) spectral width for stratiform disdrometer classifications that exceed 20 min. The bottom panel contains profiles of (d) mean equivalent reflectivity, (e) mean Doppler velocity, and (f) mean spectral width when the duration of the disdrometer stratiform classification is less than 5 min.

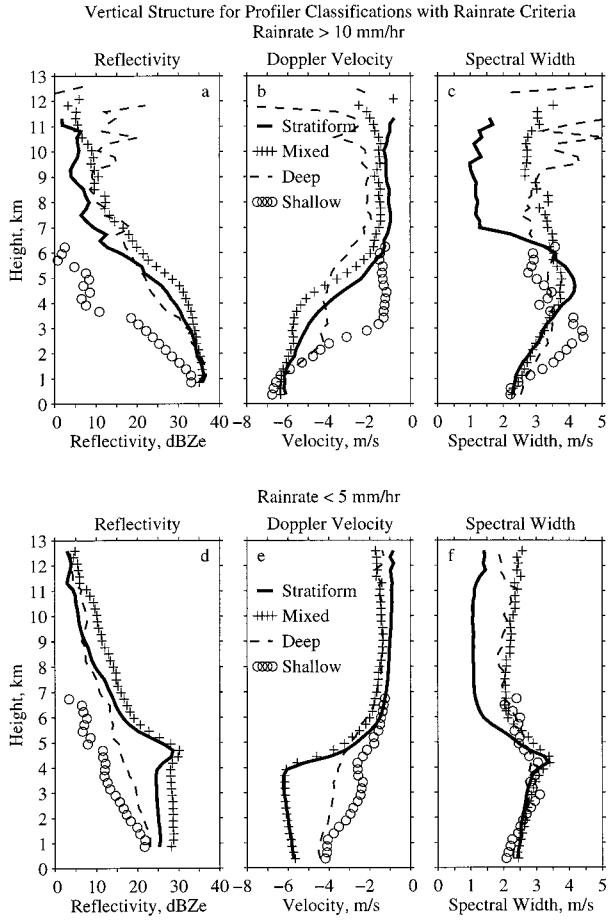

FIG. 11. Vertical structure for profiler classifications as a function of rain rate determined from the disdrometer. The top panel contains profiles of (a) mean equivalent reflectivity, (b) mean Doppler velocity, and (c) mean spectral width when the rain rate exceeds 10 mm h^{-1}. The bottom panel contains profiles of (d) mean equivalent reflectivity, (e) mean Doppler velocity, and (f) mean spectral width when the rain rate is less than 5 mm h^{-1}.

categories, as can be seen for the case studies presented in section 5.

To illustrate the fact that a substantial number of profiler-determined stratiform cases are more appropriately classified as convective, we examine the dependence of profiler classification on rain rate shown in Fig. 11. The profiler classified 59 samples of stratiform precipitation with a rain rate in excess of 10 mm h^{-1}. However, the stratiform reflectivity profiles for these cases show no BB and resemble the reflectivity profiles of the 21 samples of deep convection that were classified by the profiler in this category. The profiler also misdiagnosed 60 samples of ''mixed'' precipitation. It is readily apparent from examination of the Doppler velocity profiles in Fig. 11b that the Doppler velocities in these cases just passed the DVG criteria currently used in the WEG algorithm. These profiles of Doppler velocity should have been classified as convective. As a consequence, the profiler-determined stratiform and mixed categories are somewhat overpopulated.

Figures 11d–f contain the profiler-determined profiles of mean equivalent reflectivity, mean Doppler velocity, and mean spectral width for rain rates less than 5 mm h^{-1}. For these smaller rain rates the stratiform precipitation is dominant, as evidenced by the fact that the profiler determined 810 samples of stratiform precipitation with rain rates less than 5 mm h^{-1}. Moreover, the reflectivity and Doppler velocity profiles for the stratiform category are very similar to what was found for the profiler classification in Figs. 8d–f. The mixed category contains 307 samples and also appears as in Figs. 8d–f. However, there are also 107 samples of deep convection and 102 samples of shallow convection with rain rates less than 5 mm h^{-1} that appear to be appropriately classified by the profiler, as judged by the shape of their reflectivity profile.

Rainfall in the mixed category can be from either convective or stratiform clouds or both. It is crucial to understand whether convective or stratiform clouds are responsible for the high total rainfall percentages and mean rain rates observed for the profiler mixed category (cf. Table 2).

The mixed precipitation category recognized in the profiler algorithm has some of the features seen in the vertical structure of convective precipitation and other features more closely related to stratiform precipitation. Specifically, the profile of mean reflectivity and mean Doppler velocity resembles the profiles for stratiform precipitation, while the spectral width above the melting level is more consistent with convective precipitation. The fact that the mean equivalent reflectivity and mean Doppler velocity for the mixed category generally exceed the corresponding values for the stratiform category implies that larger drops are present in the mixed regime. Since the mixed regime often shows a well-developed melting layer signature, we conclude that the dominant type of precipitation associated with the mixed category is stratiform in nature. We interpret the mixed category as arising from the transition from convective cells with strong vertical motions to mature stratiform conditions with suppressed vertical air motions. In other words, the vertical air motions are still appreciable for the mixed category, but the microphysics is similar to stratiform precipitation microphysics. Since the mixed category arises in the transition stage of developing mesoscale convective systems, it is very likely that its horizontal structure may be much more variable than the more uniform horizontal structure normally associated with the mature phases of stratiform precipitation. For this reason it is likely that much of the mixed category precipitation seen by the profiler will be classified as convective by current scanning radar classification algorithms. Future studies will focus on this issue.

9. Conclusions

The results of precipitation classification algorithms based on the surface DSD spectra of a disdrometer and

the vertical structure of Doppler velocity and spectral width derived from the Doppler spectra of a vertically pointing wind profiler have been compared to one another. Convective regimes in the profiler algorithm include shallow convection, deep convection, and an unknown percentage of mixed cases. Stratiform regimes are the combination of stratiform and the remaining mixed cases. Overall, the profiler predicts more stratiform precipitation than the disdrometer in terms of both occurrence and rainfall. This is due to the combination of two effects: The DVG of 2 m s^{-1} km^{-1}, originally used in 30-min-averaged data, is probably a lower-bound threshold for stratiform rain. Considering the time–space ambiguity, it takes about 15 min or longer for the hydrometeors detected at around melting level to reach to the surface. Therefore, there are times when the profiler observes the BB, while the disdrometer still classifies convective rain.

Case studies show a reasonable agreement between the two algorithms. The presence of a bright band with a large DVG is well matched with the stratiform rain classification at the surface. Convective rain from the disdrometer, on the other hand, is mostly classified as deep convective, mixed, and stratiform by the profiler. The mixed cases may be attributed to convective rain in the presence of a small DVG. Some stratiform cases from the profiler also show relatively small DVGs with Doppler velocities less than 3 m s^{-1} during convective rain at the surface, indicating that the threshold derived for 30-min data is not appropriate for instantaneous observations.

The vertical structure determined from profiler observations is very useful in diagnosing tropical precipitation type. Generally, the vertical profiles of mean equivalent reflectivity, mean Doppler velocity, and mean spectral width are similar for stratiform and convective classifications by the profiler and disdrometer. Similarly, the disdrometer classifications are useful in diagnosing problems with the profiler classification algorithm. Specifically, it has been shown that the DVG criteria used in the profiler classification scheme do not always differentiate well between stratiform and convective precipitation. In the near future we plan to modify the profiler algorithm to better differentiate between stratiform and convective precipitation. The modification of the profiler algorithm will include the use of the reflectivity profile to identify the bright band signature as well. The refined profiler algorithm will be compared again with the disdrometer dataset used here to quantify the improvement.

In analyzing the 1-min disdrometer classifications we have found that at times the disdrometer classification vacillates between stratiform and convective categories. We have demonstrated that requiring the stratiform classification by the disdrometer to persist for at least 20 min yields a robust stratiform classification. Twenty minutes is long enough to eliminate much of the time–height ambiguity that invariably arises from comparisons between surface precipitation and stratiform precipitation falling from melting layers near 5 km.

By examining the vertical structure of the precipitating clouds stratified by rainfall rate we find that almost all rates exceeding 10 mm h^{-1} are associated with convective clouds. This fact suggests that an improvement to the profiler algorithm can easily be made by classifying all cases of high equivalent reflectivity at the lower levels as convective. In this connection we note that convective precipitation is almost invariably associated with increasing reflectivity with decreasing altitude, while stratiform precipitation has a more uniform vertical reflectivity profile below the melting level.

The Kapingamarangi Atoll site did not have scanning radar coverage, except for two weeks in early November from the R/V *Keifu-Maru* (Mori 1995), which may help provide further clarification of the precipitation algorithms. For example, classification algorithms applied to horizontal reflectivity fields are available (Churchill and Houze 1984; Steiner et al. 1995). A study regarding intercomparison of precipitation-type algorithms employing DSD and vertical and horizontal radar reflectivity information should be pursued in the future.

Finally, determining the altitude variation of drop size distributions is fundamental to programs like TRMM. Profilers can be used to determine the altitude variation of drop size distributions when air motions can be obtained simultaneously. The use of collocated VHF and UHF profilers has already been demonstrated as enabling the determination of the altitude distribution of the drop size distributions (Currier et al. 1992; Maguire and Avery 1994). Research is in progress to attempt the simultaneous retrieval of both clear air and precipitation information from a single profiler.

Acknowledgments. Thanks to Mr. Otto Thiele of the TRMM Office at NASA/Goddard Space Flight Center for his vision and efforts in providing for the disdrometer and other rainfall observations during TOGA COARE. Discussions with Dr. Brad Ferrier of NASA/Goddard Space Flight Center were very helpful at different stages of this research. Mr. Brad Fisher of the TRMM Office helped in analyzing the rain gauge data.

REFERENCES

Adler, R. F., and A. J. Negri, 1988: A satellite infrared technique to estimate tropical convective stratiform rainfall. *J. Appl. Meteor.*, **27,** 30–51.

Battan, L. J., 1973: *Radar Meteorology.* 2d ed. University of Chicago Press, 161 pp.

Beard, K. V., and A. Tokay, 1991: A field study of small raindrop oscillation. *Geophys. Res. Lett.,* **18,** 2257–2260.

Carter, D. A., K. S. Gage, W. L. Ecklund, W. M. Angevine, P. E. Johnston, A. C. Riddle, J. Wilson, and C. R. Williams, 1995: Developments in lower tropospheric wind profiling. *Radio Sci.,* **30,** 977–1001.

Churchill, D. D, and R. A. Houze Jr., 1984: Development and structure of winter monsoon cloud clusters on 10 December 1978. *J. Atmos. Sci.,* **41,** 933–960.

Currier, P. E., S. K. Avery, B. B. Balsley, and K. S. Gage, 1992: Combined use of 50 MHz and 915 MHz wind profilers in the estimation of raindrop size distributions. *Geophys. Res. Lett.,* **19,** 1017–1020.

Ecklund, W. L., K. S. Gage, and C. R. Williams, 1995: Tropical precipitation studies using a 915-MHz wind profiler. *Radio Sci.,* **30,** 1055–1064.

Ferrier, B. S., W.-K. Tao, and J. Simpson, 1995: A double-moment multiple-phase four-class bulk ice scheme. Part II: Simulations of convective storms in different large-scale environments and comparisons with other bulk parameterizations. *J. Atmos. Sci.,* **52,** 1001–1033.

Gage, K. S., C. R. Williams, and W. L. Ecklund, 1994: UHF wind profilers: A new tool for diagnosing tropical convective cloud systems. *Bull. Amer. Meteor. Soc.,* **75,** 2289–2294.

——, ——, and ——, 1996: Application of the 915-MHz profiler for diagnosing and classifying tropical precipitating cloud systems. *Meteor. Atmos. Phys.,* **59,** 141–151.

Hartmann, D. L., H. H. Hendon, and R. A. Houze Jr., 1984: Some implications of the mesoscale circulations in tropical cloud clusters for large-scale dynamics and climate. *J. Atmos. Sci.,* **41,** 113–121.

Heinrich, W., J. Joss, and A. Waldvogel, 1996: Raindrop size distributions and the radar bright band. *J. Appl. Meteor.,* **35,** 1688–1701.

Houze, R. A., Jr., 1989: Observed structure of mesoscale convective systems and implications for large-scale heating. *Quart. J. Roy. Meteor. Soc.,* **115,** 425–461.

——, 1993: *Cloud Dynamics.* Academic Press, 573 pp.

Kodaira, N., and J. Aoyagi, 1990: History of radar meteorology in Japan. *Radar in Meteorology,* D. Atlas, Ed., Amer. Meteor. Soc., 69–76.

Kozu, T., and K. Nakamura, 1991: Rainfall parameter estimation from dual-radar measurements combining reflectivity profile and path-integrated attenuation. *J. Atmos. Oceanic Technol.,* **8,** 259–271.

Kummerow, C., I. M. Hakkarinen, H. F. Pierce, and J. A. Weinman, 1991: Determination of precipitation profiles from airborne passive microwave radiometric measurements. *J. Atmos. Oceanic Technol.,* **8,** 148–158.

Maguire, W. B., II, and S. K. Avery, 1994: Retrieval of raindrop size distributions using two Doppler wind profilers: Model sensitivity testing. *J. Appl. Meteor.,* **33,** 1623–1635.

Mapes, B., and R. A. Houze, 1993: An integrated view of the 1987 Australian monsoon and its mesoscale convective system. II: Vertical structure. *Quart. J. Roy. Meteor. Soc.,* **119,** 733–754.

Mori, K., 1995: Equatorial convection observed by the research vessel *Keifu-Maru* during the TOGA COARE IOP, November 1992. *J. Meteor. Soc. Japan,* **73,** 491–508.

Rogers, R. R., I. I. Zawadski, and E. E. Gossard, 1991: Variation with altitude of the drop-size distribution in steady light rain. *Quart. J. Roy. Meteor. Soc.,* **117,** 1341–1369.

Rosenfeld, D., E. Amitai, and D. B. Wolff, 1995: Classification of rain regimes by the three-dimensional properties of reflectivity fields. *J. Appl. Meteor.,* **34,** 198–211.

Simpson, J., R. F. Adler, and G. R. North, 1988: A proposed Tropical Rainfall Measuring Mission (TRMM) satellite. *Bull. Amer. Meteor. Soc.,* **69,** 278–295.

Steiner, M., R. A. Houze Jr., and S. E. Yuter, 1995: Climatological characterization of three-dimensional storm structure from operational radar and rain gauge data. *J. Appl. Meteor.,* **34,** 1978–2007.

Tao, W.-K., J. Simpson, S. Lang, M. McCumber, R. Adler, and R. Penc, 1990: An algorithm to estimate the heating budget from vertical hydrometer profiles. *J. Appl. Meteor.,* **29,** 1232–1244.

——, S. Lang, J. Simpson, and R. Adler, 1993: Retrieval algorithms for estimating the vertical profiles of latent heat release: Their applications for TRMM. *J. Meteor. Soc. Japan,* **71,** 685–699.

Tokay, A., and D. A. Short, 1996: Evidence from tropical raindrop spectra of the origin of rain from stratiform versus convective clouds. *J. Appl. Meteor.,* **35,** 355–371.

Waldvogel, A., 1974: The N_0 jump of raindrop spectra. *J. Atmos. Sci.,* **31,** 1068–1078.

Williams, C. R., W. L. Ecklund, and K. S. Gage, 1995: Classification of precipitating clouds in the Tropics using 915-MHz wind profilers. *J. Atmos. Oceanic Technol.,* **12,** 996–1012.

Willis, P. T., and P. Tattleman, 1989: Drop-size distributions associated with intense rainfall. *J. Appl. Meteor.,* **28,** 3–15.